Fabrication of iron-coated activated carbon and its application for phosphorus removal from aqueous solution

Bayuh Abuhay Kibret, [*,] Ye Wu[*,**] Mengist Minale Tashu[*,**]**

[*] College of Environmental Science and Engineering, State Key Laboratory of Pollution Control and Resource Reuse, Tongji University, Shanghai 200092, P.R. China
[**] Shanghai Institute of Pollution Control and Ecological Security, Shanghai 200092, P.R. China

DOI: 10.29322/IJSRP.10.05.2020.p10110
http://dx.doi.org/10.29322/IJSRP.10.05.2020.p10110

Abstract- In this paper, we report a facile co-precipitation method to synthesize a low-cost iron impregnated activated carbon (Fe-CAC) for phosphate removal from aqueous solution. The result shows that Fe-CAC has high phosphate adsorption capacity than pristine activated carbon (CAC). Both Fe-CAC and CAC adsorbents reached equilibrium at 9 h with the maximum phosphate adsorption capacity of 216.6 and 173.2 mg/g P, respectively. The adsorption capacity of phosphate onto Fe-CAC was high in acidic solution (216.6 mg/g at pH = 4), while decreased in alkaline solution (168.9 mg/g at pH = 12). This is owing to the mechanism that was governed by electrostatic attraction and the exchange of ligands at low pH. The phosphate adsorption capacity increased as temperature increases onto Fe-CAC. The Fe-CAC adsorbent has a rapid adsorption process (92%) in the first one hour. Phosphate adsorption kinetics on Fe-CAC adsorbent go thoroughly along with a pseudo-second-order kinetics model, attributing that chemical sorption regulated the method. The Langmuir isotherm model had a better description of the phosphate adsorption process than the Freundlich isotherm model. The presence of magnetite (Fe_3O_4) on the activated carbon surfaces contributes to the high capacity and selectivity of phosphate species adsorption. The Fe-CAC has significantly sustainable regeneration capability while repeatedly being used in aqueous solution for phosphate removal. Fe-CAC adsorbent shows excellent performance in the adsorption as well as in desorption processes in the aqueous solution, which is promising for the practical application.

Index Terms- Commercial Activated Carbon; Iron Impregnated Activated Carbon; Adsorption; Phosphorous Removal; Regeneration

I. INTRODUCTION

Excess discharge of nutrients (especially, phosphorus and nitrogen) in water bodies has accelerated the outbreak of eutrophication and promoted the expansion of harmful algal blooms [1, 2]. These algal blooms pose a severe threat to water pollution, oxygen depletion, and the sustainability of aquatic ecosystems. Various researchers reported that phosphorus has a great impact to promote eutrophication on lakes, rivers, and seas than other nutrients [3, 4]. For this reason, it is important to control the amounts of phosphorous in water bodies to maintain the water quality and a green environment for the forthcoming generation. Above 0.02 mg/L concentration of phosphate was responsible to enable the presence of eutrophication in rivers and lakes [1]. To protect the excess flow of these nutrients (phosphate) into streams and lakes, the United States Environmental protection authority approves 0.05 and 0.1 mg/L of total phosphorus, respectively [5]. Recently, several treatment technologies are applied for wastewater treatments, which are mainly categorized into biological, chemical precipitation, and adsorption [6, 7]. However, chemical precipitation methods face difficulties with incurring a high cost, production of secondary pollution, and inefficient for removal of trace phosphorus concentration. Biological methods have also unstable efficiency because these techniques are often requiring continuous monitoring and susceptible to operational difficulties [8, 9]. On the other hand, adsorption is considered the most promising technology for the removal of phosphorus, which requires little initial cost, land, and simple design during application [10-12].

At the moment, several adsorbents have been developed and investigated for phosphate removal [13-15]. Nevertheless, virgin activated carbon [16, 17], magnetic iron oxide nanoparticles [18], Fe_3O_4 nanoparticles [19], calcium-silicate material [20], iron-coated natural and engineered sorbents [21], straw biochar [7], zirconium modified activated carbon nanofiber [10], iron-impregnated granular activated carbon [22], biochar derived from peanut shell [23], modified biochar [6], activated carbon fiber loaded with lanthanum oxide [3], zeolite, calcite, and bentonite [24], fly ash [4] treated aluminum waste-filings [18, 25] exhibit little binding affinity, poor regeneration capability, low adsorption capacity, and poor kinetics towards phosphorus adsorption. Iron had high selectivity and affinity towards phosphorus species in the adsorption process [11]. Therefore, impregnation of iron with pristine activated carbon through the co-precipitation method by heating $FeCl_3 \cdot 6H_2O$ and $FeSO_4 \cdot 7H_2O$ solution at 70 °C for 20 minutes before adding CAC would improve the limitation of the above adsorbents towards phosphate adsorption. The presence of large surface area, a high degree of surface reactivity, and adaptable pore size distribution are among the important characteristics which make iron impregnated activated carbon viable for this purpose.

Hence, the main objective of this study was intended for the preparation of highly cost-effective and high phosphate-binding affinity adsorbent through the co-precipitation method (precipitated iron (II) hydroxides to the surfaces of commercial activated carbon). The newly prepared Fe-CAC and pristine CAC adsorbents were analyzed using BET for pore size and surface area, SEM for surface morphology, and XRD for the adsorbent's crystallization structure. Moreover, the effect of different adsorption parameters, phosphate adsorption isotherms, kinetics, and thermodynamics was examined.

II. Materials and Methods

1.1. Chemicals

Iron (III) chloride hexahydrate ($FeCl_3.6H_2O$), ferrous (II) sulfate heptahydrate ($FeSO_4•7H_2O$), commercial activated carbon (CAC), potassium dihydrogen phosphate (KH_2PO_4), sulfuric acid (H_2SO_4), antimony potassium tartrate ($C_4H_4O_6K•SbO•1/2H_2O$), ammonium molybdate tetrahydrate ($(NH_4)_6Mo_7O_{24}•4H_2O$), ascorbic acid ($C_6H_8O_6$) were used for the experiment. All the above reagents were used in analytical grade and purchased from Sino pharm chemical reagent Ltd. Synthetic phosphorus solution used for adsorption kinetics and isotherm was prepared by dissolving 4.4 g of KH_2PO_4 in 1 L of deionized water, which corresponds to 1000 mg /L P. Desired solutions were prepared by dilution of the stock solution. The pH solution was adjusted to neutral by adding 0.1 M NaOH and HCl dropwise. Deionized water was used to prepare all solutions in the whole experiment of this study.

1.2. Adsorbent preparation

Chemical activation of commercial activated carbon was conducted using iron (III) chloride hexahydrate ($FeCl_3.6H_2O$) and ferrous (II) sulfate heptahydrate ($FeSO_4·7H_2O$). Iron impregnated commercial activated carbon was prepared through the co-precipitation method [12]. Accordingly, 3.9 g of $FeCl_3·6H_2O$ and 7.8 g of $FeSO_4·7H_2O$ was dissolved with 400 mL distilled water into 500 mL beaker. The mixture was stirred and heated at 70°C for 20 minutes. Subsequently, 10 g of CAC was added into the solution (with the mass ratio of 1.2**:** 5) and stirred continuously for 5 hours. During stirring, NaOH solution (0.1 M) was added drop-wise into the solution until the pH reached to 12, and precipitate iron (II) hydroxides to the surfaces of CAC from the aqueous solution. Following freezing the solution, Fe-CAC was washed with deionized water till the pH of the filtrate reached neutral and become dried in an oven at 80°C for overnight. Finally, the newly prepared Fe-CAC and CAC were designated as Fe-CAC and CAC, respectively. the schematic illustration is shown in Fig.1

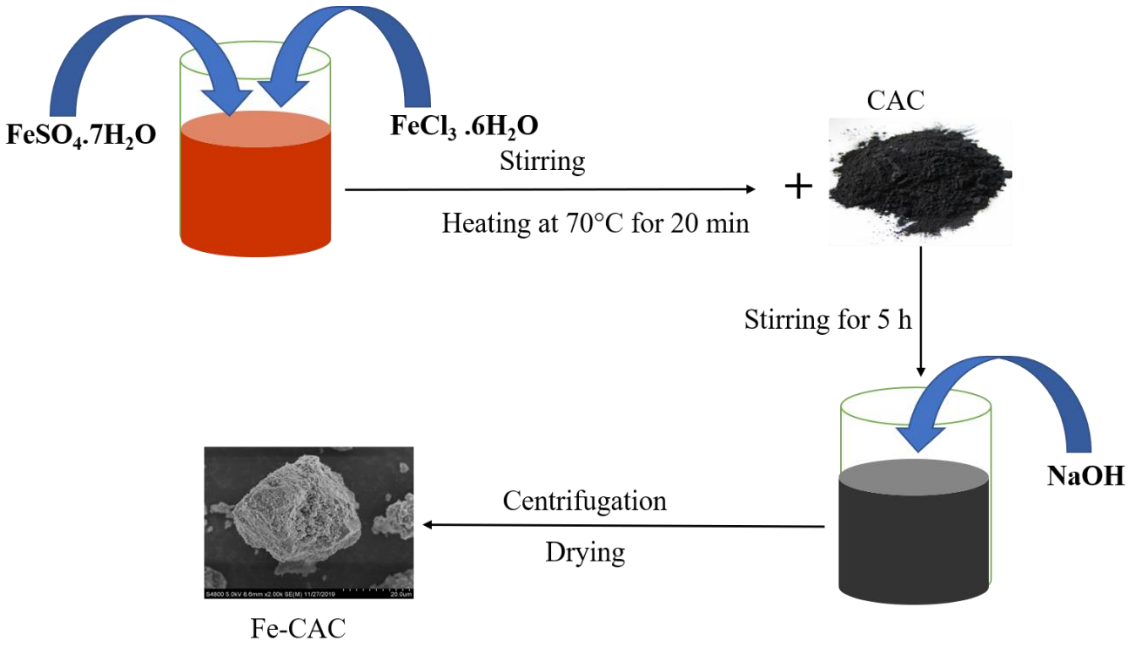

Figure.1: Schematic illustration of the preparation of Fe-CAC adsorbent

.

1.3. Adsorbent Characterization

The surface area and pore volume of CAC and Fe-CAC were measured by using Brunauer–Emmett–Teller (BET) surface area and porosity analyzer, including the adsorption-desorption isotherm of N_2 at 77 K. To investigate the surface morphologies of CAC and Fe-CAC were examined by a scanning electron microscope (SEM). The crystallization structure of the virgin activated carbon and prepared composite adsorbent were analyzed via XRD.

1.4. Phosphate adsorption batch experiments

The adsorption capacity of phosphate with CAC and prepared iron impregnated in aqueous solution was conducted through a batch experiment. As the procedure reported by [12]. Adsorption isotherm was examined by adding 0.05 g of the iron-loaded activated carbon into 100 mL flasks containing 50 mL solution with different phosphate ion concentrations (50, 100, 150, 200, 250 mg/L). Subsequently, the pH of the sample solution was adjusted to 4 and shake in at 200 rpm for 9 hours. After settling,

the supernatant was filtered through the suspension was immediately filtered through a 0.45 µm membrane using the syringe, and then analyzed on UV–vis spectrophotometer using the ascorbic acid method [26]. The capacity of phosphate adsorption at equilibrium and removal efficiency (E, %) were calculated based on Eq. (1) and Eq. (2)

$$q_e = (C_0 - C_e) \times \frac{V}{m} \quad (1)$$

$$E = \frac{C_0 - C_e}{C_0} x\ 100 \quad (2)$$

where q_e is the equilibrium adsorption capacity of both Fe-CAC and CAC samples(mg/g), V is the volume of solution (mL), C_e and C_o represent the concentrations at the equilibrium and initial time (mg/L), respectively, and m is the weight of adsorbent (g).

A kinetic study was conducted by adding 0.05 g of Fe-CAC and CAC in 100 mL bottle containing 50 mL solution with 250 mg/L phosphate solution; the pH of the solution was adjusted to 4 with 0.1 M NaOH or 0.1 M of HCl. The solution was stirred on the magnetic stirrer at room temperature, and the samples were taken at different contact times (0, 30, 60, 180, 360, 540, and 720 minutes) to examine the residual phosphate concentration on UV–vis spectrophotometer (UV-2600 SHIMADZU) using the ascorbic acid method. The influence of pH on adsorption capacity of phosphate for both adsorbents was examined at pH (2, 4, 6, 7, 8, 10, and 12) in 250 mg/L phosphate concentration. The effect of initial phosphate concentration on adsorption capacity was studied for both adsorbents at different phosphate concentrations (50, 100, 150, 200, 250 mg/LP). The effect of temperature on phosphate adsorption capacity of both adsorbents was also studied at different temperatures (298, 308, 318, and 328 K).

III. Results and Discussion

1.5. Characterization of adsorbents

XRD analysis was performed for both CAC and Fe-CAC samples to provide details on the crystalline structures. The patterns of XRD for both adsorbents are shown in Fig. 2 (a). The CAC had no intense peak, suggesting that the amorphous nature of the carbon material. Changes in the diffraction pattern of Fe-CAC adsorbents have been observed, likely because iron is well impregnated on the surface of the CAC (Wang et al., 2011). The peaks shown at 25° and 43° were confirmed the appearance of a carbonaceous structure on the commercial activated carbon surface (Altıntıg et al., 2017). As illustrated in Fig. 2 (a). the major peaks (2-theta = 30.18°, 35.5°, 57.15°, and 62.76°) were formed after impregnation of iron-loaded activated carbon, corresponding to the peaks of magnetite (Fe_3O_4) (Long et al., 2011; Wang et al., 2011). In general, these findings revealed that adsorbent with magnetic properties was impregnated with the existence of major components of magnetic iron.

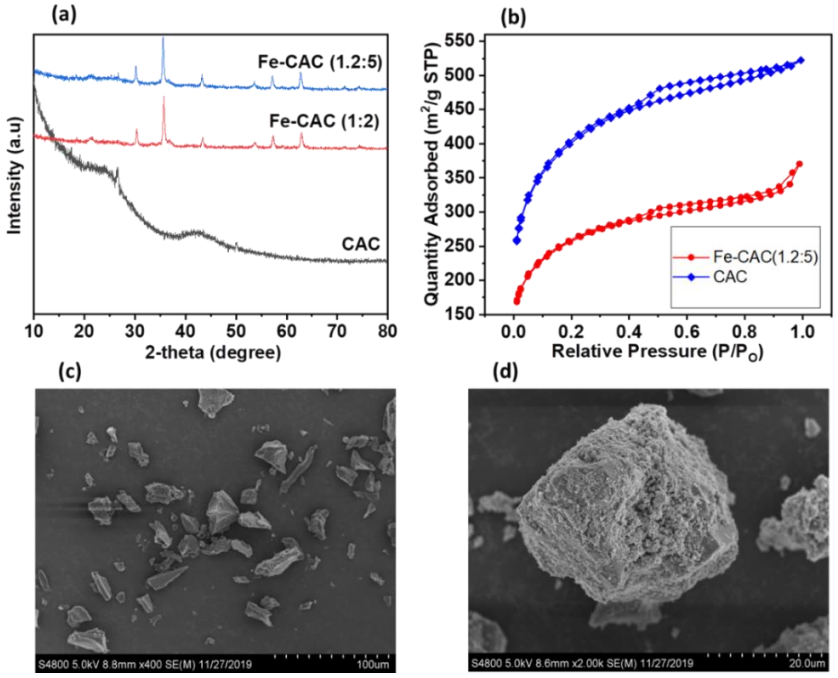

Figure. 2: XRD results of (a) CAC and Fe-CAC, (b) The N_2 adsorption-desorption isotherms of Fe-CAC (1.2:5) and CAC, SEM results of (c) CAC, and (d) Fe-CAC.

The surface and porous properties of the as-synthesized adsorbents were described in Fig. 2(b). As shown in Fig. 2(b), the surface area of pure commercial activated carbon without any modification was (1450.28 m^2/g), which can be substantially reduced after iron solution impregnation (929.86 m^2/g). Nevertheless, the newly modified iron adsorbent exhibits greater total pore volume and average pore diameter, resulting in sufficient adsorption capacity. The surface area of Fe-CAC was further decreased after being treated with the iron solution, which is due to iron being occupied in the surface and pores of the

commercial activated carbon. This impregnation significantly improves the selectivity and binding affinity to phosphorus species in the adsorption cycle, that had been in favor of improving Fe-CAC adsorbent adsorption capability [14]

The N_2 adsorption-desorption isotherms of Fe-CAC and CAC were investigated as shown in Fig. 2 (b). The adsorption process of the N_2 gas Fe-CAC and CAC solid surface of adsorbents phenomena was physio-sorption. It happens when gas adsorption is carried into an exchange with the surface of a solid (the adsorbent). The intermolecular forces were involved in the same kind as those responsible for the imperfection of real gases and the condensation of vapors [27]. According to IUPAC classification, CAC displayed a combined isotherm type I with an H_4 hysteresis loop, explaining the presence of a narrow slit-like microporous and mesoporous surface gain through multilayer adsorption followed by capillary condensation. Fe-CAC displayed isotherm type I and II with an H_4 loop look to be associated with narrow slit-like pores [28]. It is noteworthy that, the BET specific surface area (S_{BET}) of CAC 1450.28 m^2/g is greater than Fe-CAC (1.2:5) 929.86 m^2/g. This is probably because of the impregnation of iron on the pores of activated carbon to increase the affinity of phosphate adsorption. However, the total pore volume and average pore diameter of Fe-CAC are greater than CAC.

The external morphology of the commercial activated carbon sample is shown in Fig. 2 (c). the surface feature of the virgin CAC was relatively smooth and flat. The surface of the newly prepared iron impregnated activated carbon samples were much coarser as shown in Fig. 2 (d). Moreover, the surface of Fe-AC was uneven and rough with abundant protuberances and lots of pores, which favored the diffusion of the phosphate to its surface. It can be found that a few salt crystals distributed over the external surfaces of the iron-doped samples. It also revealed that iron oxide particles were much more uniformly deposited on the surface of the activated carbon. This could be attributed to the reason that Fe (II) should be able to diffuse into the internal pores of activated carbon.

1.6. Effect of initial concentration on phosphate adsorption

To understand the effect of initial phosphate concentration on the phosphate adsorption capacity, 0.05 g adsorbent was added to 50 mL of solutions with various initial phosphate concentrations (50, 100, 150, 200, and 250 mg P/L) at room temperature in the batch adsorption experiments**.** The results were explained in Fig. 3 (a). It clearly showed that the amount of phosphate adsorption capacity increased with the increases of initial phosphate concentration, this is because the newly prepared iron impregnated activated carbon (Fe-CAC) and CAC adsorbents have sufficient active sites competent for a relatively high concentration of phosphate. However, phosphate removal efficiency as described in Fig. 3(a) decreases with the increasing of initial phosphate concentration owing to the adsorption sites on both adsorbents surface that were gradually occupied by adsorbed phosphate, resulting in a decrease of the remaining sites for the adsorption of phosphate**.** An increase in the initial phosphate concentration (C_o) led to a prominent decrease in the percentage removal of phosphate in both adsorbents. The result indicates that Fe-CAC had a higher phosphate removal capacity and efficiency than CAC**.**

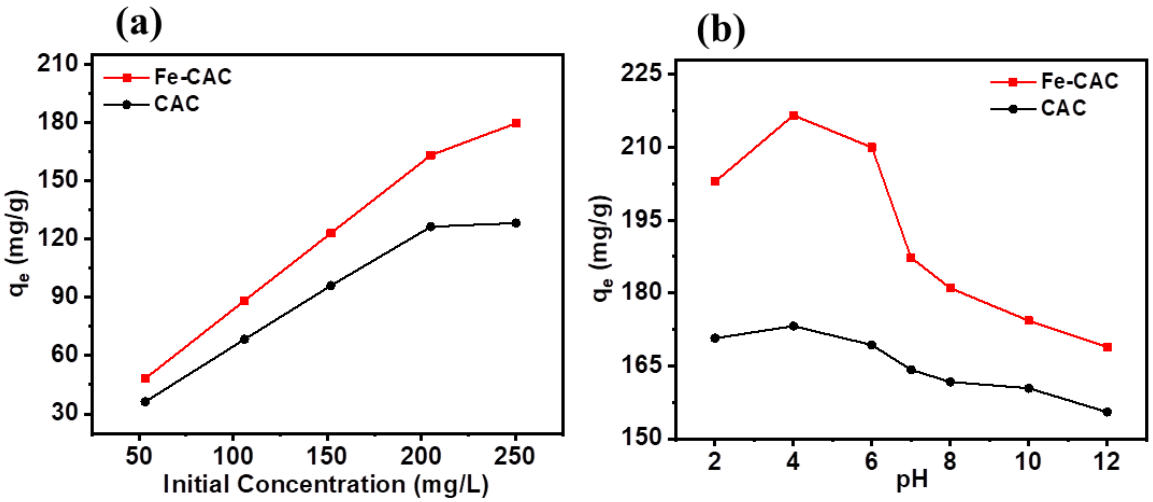

Figure 3: (a) Effect of initial concentration (initial concentration: 50-250 mg/L, pH: 4, temperature: 298 K, contact time: 9 hrs., agitation speed: 200 rpm, and adsorbent dosage 0.05 g) and (b) effect of pH on phosphate adsorption (initial concentration: 250 mg/L, pH: 2-12, temperature: 298 K, contact time: 9 hrs., agitation speed: 200 rpm, and adsorbent dosage: 0.05 g).

1.7. Effect of pH

The effect of pH on phosphate adsorption was investigated from pH 2 to 12. The experimental findings are listed in Fig. 3(b). It showed phosphate uptake was highly pH-dependent. From pH 2 to 4, the phosphate uptake for both Fe-CAC and CAC first increased rapidly with the pH-value increases, then gradually decreased until pH 6. After pH > 6, the phosphate uptake capacity of phosphate decreases with the rise of pH. The maximum phosphate adsorption capacity was achieved at pH 4, which was 216.6 mg/g. A similar study [29] confirms that the maximum phosphate adsorption capacity was achieved under acidic conditions and decreased with an increase in pH value which is consistent with this work. The newly prepared Fe-CAC adsorbent surface is charged positively with the presence of more H^+ ions in

the adsorbent's surrounding surfaces at the lowest pH level, resulting in stronger adsorption of phosphate ions to the adsorbent surface (Wang et al., 2011). Immediately, H^+ ions and phosphate molecules surrounded the active sites on the surface of the Fe-CAC. Iron impregnated activated carbon products have high reactivity and selectivity through electrostatic forces to phosphate species. Such electrostatic forces improve the binding of negatively charged phosphate molecules to the surface of positively charged Fe-CAC adsorbent, leading to the high amount of phosphate adsorbed on Fe-CAC at pH 4 (216.6 mg/g) relative to CAC surface. Theoretically, at pH 2.15-7.20, the dominant form of P in solution is H_3PO_4 and $H_2PO_4^-$ and the main form changes to HPO_4^{2-} when pH is between 7.2 and 12.33. So, H_3PO_4 and $H_2PO_4^-$ are the main species of phosphate at low pH, and $H_2PO_4^-$ is the main ion to attract the adsorption site on both adsorbents. Besides, ligand exchange between the unprotonated $H_2PO_4^-$ and the OH^- existed on the surface of Fe-CAC, is recognized as a promising mechanism for phosphate adsorption [27, 30].

The OH^- ions can restrict the interaction between the anion phosphate molecules ($H_2PO_4^-$) and the Fe-AC surface under alkaline conditions, where the high concentration of OH^- competes with phosphate for the adsorption position. Besides, Fe-CAC's surface was negatively charged with increased surrounding OH^- with the rise of pH, which strengthened the electrostatic repulsion between phosphate and adsorbents, leading to weak adsorption of phosphate. From this experiment, the pH has a significant effect on the activated carbon and phosphate species exchanges of newly prepared iron impregnated species since it affects numerous factors such as phosphate speciation, iron oxide surface charge, and iron oxide solubility, and the complex formed iron with phosphate. As pH increases in the surface of the newly prepared iron impregnated activated carbon adsorbent, as well as the surrounding ions, there will possibly be more negative and electrostatic repulsion that reduces the adsorption of phosphate. As shown in Fig. 3(b), the efficiency of phosphate removal was high in acidic conditions as a result of electrostatic force and decreased because of electrostatic repulsion as pH increases in an alkaline state.

1.8. Effect of contact time

The removal of phosphate by Fe-CAC and CAC as a function of time with different contact times (0, 30, 60, 180, 360, 540 and 720 minutes) with initial phosphate concentration 250 mg/L and under pH 4, were illustrated in Fig. 4. It was notable that the two curves exhibit the same trend. The amount of phosphate uptake increased rapidly in the early stage of the phosphate adsorption reaction process, possibly due to the availability of abundant active sites on the Fe-CAC and CAC adsorbent surfaces. meanwhile, the phosphate uptake rate developed slower as a result of the decrease of active sites with contact time. In this study, 92% of the phosphate adsorption reaction was performed within one hour, which pronounces the reaction of phosphate species with the newly prepared adsorbent was fast in the early stage. The same result was explained by the previous study [10]. After 180 min, the phosphate adsorption capacity increases slowly through time until the equilibrium adsorption capacity was attained.

Therefore, the contact time 720 minutes was enough to attain the equilibrium adsorption. It was taken as a contact time for the whole experiment. The equilibrium phosphate adsorption capacity values q_e on the newly prepared Fe-CAC, adsorbent and phosphate remained in the equilibrium solution (C_e) at 298, 308, 318, and 328 K was estimated to be 192.8, 202.6, 205.1, 207.8 mg/g and 55.3, 45, 42.9, 41.2 mg/L, respectively.

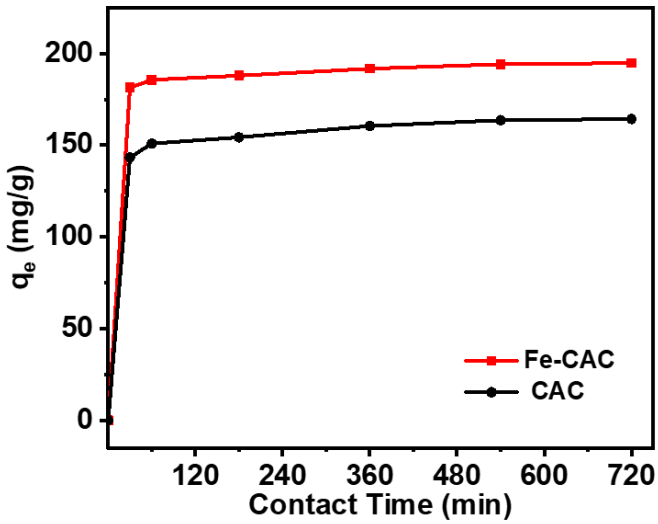

Figure 4: Effect of contact time on phosphate adsorption (initial concentration: 250 mg/L, pH: 4, Temperature: at room temperature, contact time: 9 hrs., adsorbent dosage 0.05g, and, agitation speed: 200 rpm).

1.9. Adsorption Isotherms

The phosphate adsorption capacity of both Fe-CAC and CAC were examined using the equation explained by [23, 27] Freundlich (Eq. (3)) and Langmuir (Eq. (4)) adsorption isotherms. The result was illustrated in Table (1).

$$q_e = K_F C_e^{\frac{1}{n}} \quad (3)$$

$$q_e = \frac{q_{max} K_L C_e}{1 + K_L C_e} \quad (4)$$

where q_e is the equilibrium phosphate adsorption capacity of both irons coated and commercial activated carbon per unit weight of adsorbent (mg/g) at an equilibrium concentration of adsorbent in an aqueous solution, C_e is the final equilibrium phosphate concentration (mg/L). K_F and K_L are Freundlich and Langmuir constants, respectively. q_{max} (mg/g) represents the maximum adsorption capacity, and 1/n is the factor of heterogeneity in the Freundlich isotherm model.

Generally, in this experiment, phosphate adsorption isotherm designates a relationship between the amount of phosphate uptake on Fe-CAC and CAC and the amount of phosphate residual in solution at equilibrium condition while maintaining temperature constant. The adsorption isotherm data were fitted to the Langmuir and Freundlich equilibrium isotherm equations. The non-linear plots of Langmuir and Freundlich isotherm model for the uptake of phosphate onto Fe-CAC and CAC were illustrated in Fig. 5 (a) and (b). The Langmuir and Freundlich isotherm non-linear fitted plot data and parameters from the model equation are summarized and presented in Table 1.

Table 1: Langmuir and Freundlich isotherm parameters of phosphate Adsorption onto Fe-CAC and CAC adsorbents

Adsorbents	Langmuir model			Freundlich model		
	q_{max} (mg/g)	K_L (L/mg)	R^2	n	K_F (L/g)	R^2
Fe-CAC	237.2	0.037	0.966	0.47	24.94	0.920
CAC	175.8	0.014	0.951	0.56	9.39	0.875

The experimental data for Fe-CAC was better described and fitted with the Langmuir isotherm model as described by R^2 values. From the Langmuir isotherm model equation (summarized in Table 1) q_{max} values for phosphate adsorption capacity were higher for Fe-CAC adsorbent as compared with the results of CAC. This value is also high as compared to the reported data in the literature (see in Table 2). By comparing the two popular isotherm models, the Langmuir equation had a stronger correlation ($R^2 > 0.966$) than the Freundlich equation ($R^2 > 0.875$). Therefore, the phosphate species adsorption reaction onto Fe-CAC is closer to a monolayer surface reaction. As stated by [9], the uptake of phosphate species onto iron oxide adsorbent was performed basically on the surface coordination between surface hydroxyl groups in iron oxide solids and phosphate ions.

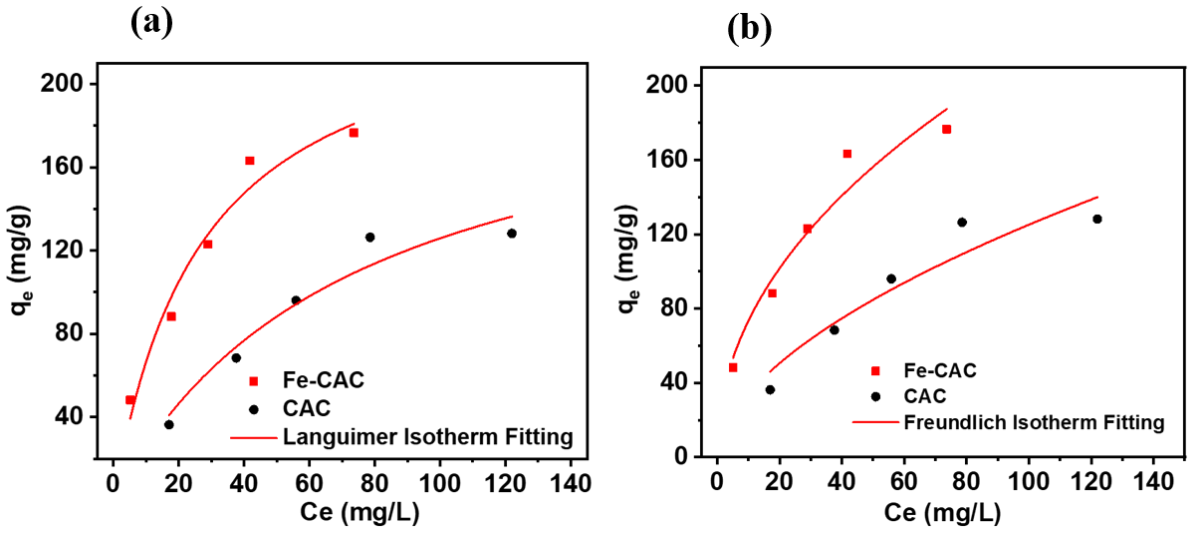

Figure 5: (a) Langmuir isotherm Fitting (b) Freundlich isotherm Fitting ((initial concentration: 50-250 mg/L, pH: 4, temperature: at room temperature, contact time: 9 hrs., adsorbent dosage: 0.05 g, and, agitation speed: 200 rpm)

Table 2: Comparison of maximum phosphate adsorption capacity of various adsorbents for phosphate removal.

Adsorbents	pH	Maximum adsorption capacity (mg/g)	Reference
Raw activated carbon	2	192.31	[31]
Fe_3O_4@GPTMS@Lys	4	185	[32]
Iron-modified biochar's	4	111	[27]

Iron oxide nanoparticles	3-6	5.03	[18]
Fe-GAC	2	10.8	[33]
Fe_3O_4 Nano-particles	2.77	3.65	[19]
Fe–Zr binary oxide	4	13.65	[34]
CAC	**4**	**173.2**	**This study**
Fe-CAC	**4**	**216.6**	**This study**

1.10. Kinetics studies on phosphate adsorption

Kinetic and equilibrium adsorption models were used to understand the interaction mechanisms between phosphate and iron-loaded activated carbon adsorbent. Adsorption dynamics of the iron-loaded activated carbon toward phosphate was measured as a function of time. For this study, the flasks were incubated in a magnetic stirrer on a water bath at 298, 308, 318 and 328 K at 200 rounds per minute. 250 mg/L phosphate concentration in 100 mL containing 50 mL solution was measured for 7 different contact times (0, 30, 60, 180, 360, 540, and 720 minutes). At the end of each contact time, the suspension was immediately filtered through a 0.45 µm membrane using the syringe, and then analyzed on UV–vis spectrophotometer using the ascorbic acid method. All the experimental treatments were performed in duplicate and the average values were reported. Additional analyses were conducted whenever two measurements show a difference larger than 10%. Two commonly used mathematical models, pseudo-first-order and pseudo-second-order, were used to simulate adsorption kinetics of phosphate onto Fe-CAC adsorbent to the rate of reaction concerning time (kinetics). To study the kinetics of phosphate onto Fe-CAC, two popular kinetic models were used, which was similar to the previous study, [18, 35] which are shown on (Eq. (6)) and (Eq. (7)), respectively.

$$q_t = q_e(1 - \exp(-k_1 t)) \quad (5)$$

$$q_t = \frac{q_e^2\, k_2 t}{1 + q_e\, k_2 t} \quad (6)$$

Where; q_t and q_e (mg/g) are the amounts of phosphate adsorbed at time t and equilibrium, respectively, and k_1 (h^{-1}) and k_2 (g/mg/h) are the first-order and second-order apparent adsorption rate constants, respectively.

To investigate the maximum phosphate adsorption capacity and recognize the possible rate-controlling steps, two popular kinetic models (pseudo-first-order and pseudo-second-order models) were applied to understand the adsorption process (on Fe-CAC). The phosphate adsorption capacity of the newly prepared adsorbents (Fe-CAC), as a function of time, is shown in Fig. 6. Based on the graph of phosphate adsorption capacity as a function of time, the adsorption of phosphate has occurred rapidly at the first 60 min, which could be attributed because of the available number of active adsorption sites onto the surfaces of the newly synthesized Fe-CAC adsorbents.

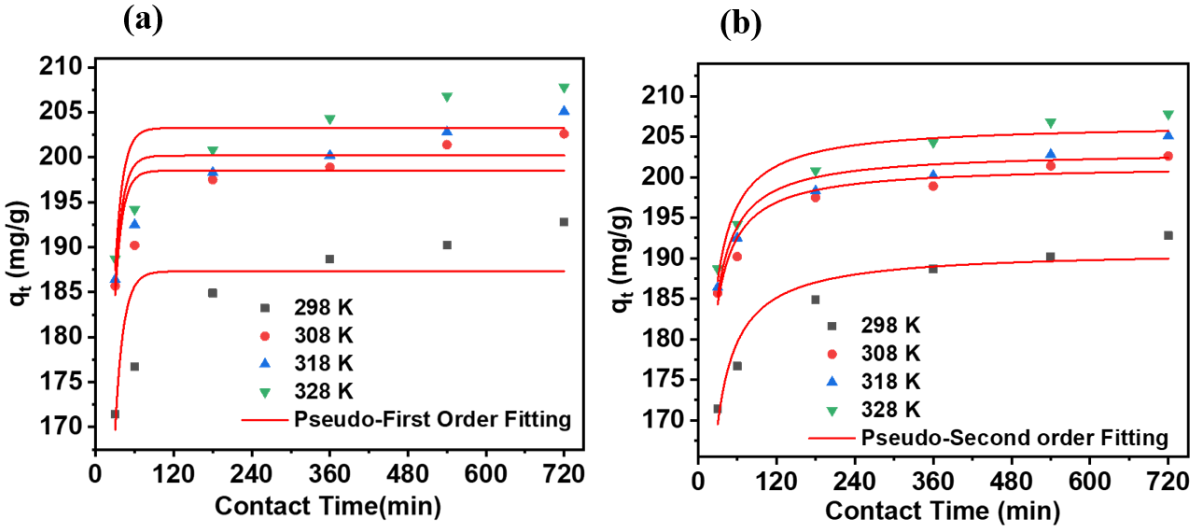

Figure 6: (a) Pseudo-First order Kinetic Fitting (b) Pseudo-Second Order Kinetic Fitting ((initial concentration: 250 mg/L, pH: 4, adsorbent dosage 0.05g, and, agitation speed: 200 rpm).

The pseudo-first-order and pseudo-second-order kinetic model parameter results are shown in Table 3. For the two kinetic models under pH 4, at different temperatures (298, 308, 318, and 328 K) and 250 mg/L initial phosphate concentration, the non-linear fitted curves were shown in Fig. 6 (a) and (b) with the experimental results.

Table 3: Kinetics model parameters for phosphate adsorption onto Fe-CAC

Temperature (K)	Pseudo-first-order model parameters			Pseudo-second-order model parameters		
	q_e (mg/g)	K_1	R	q_e (mg/g)	K_2	R^2
298	187.311	0.079	0.631	190.965	0.00138	0.92897
308	198.510	0.085	0.636	201.475	0.00156	0.93368
318	200.185	0.087	0.639	203.192	0.00171	0.93573
328	203.258	0.089	0.673	206.587	0.00178	0.93872

Based on the result shown in Table 3, the values of correlation coefficients (> 0.93) for the pseudo-second-order kinetic model was higher than the pseudo-first-order kinetic models. Consequently, the pseudo-second-order kinetic model equation is the one that well describes the phosphate adsorption kinetics on Fe-CAC. From the above results, we can conclude that the overall phosphate adsorption process on Fe-CAC was governed by chemisorption, which suggests that the overall rate of phosphate sorption processes is controlled by the chemisorption's, through the exchange of electrons between Fe-CAC adsorbent and phosphate ions with electrostatic forces. Similar results predominantly with the pseudo-second-order kinetic model indicate chemisorption [14, 28, 30]. As shown in Fig. 6 (b) and the results in Table 3, the maximum phosphate adsorption capacity results from the curves fitted by the pseudo-second-order kinetic model for the four different temperature and 250 mg/L initial phosphate concentration were very close to the experimental results. This also shows that the pseudo-second-order kinetic model bounces a reasonable simulation for the phosphate removal process on Fe-CAC adsorbent.

1.11. Effect of temperature

Fig. 7 designates the plot of phosphate adsorption capacity versus contact time of solution of Fe-CAC at different temperature 298, 308, 318, and 328 K by keeping the initial phosphate concentration at 250 mg/L. The equilibrium phosphate adsorption capacity, q_e (mg/g) of Fe-CAC increases with the increasing temperature from 298 to 328 K. The amount of phosphate adsorption increases from 190.9 to 206.6 mg/g while increasing the temperature from 298 to 328 K, respectively. For this experiment, employing different temperatures of solution plays a substantial role in the phosphate uptake process within the newly prepared adsorbents. As the temperature rises, the viscosity of the solution decreases, which ensures increasing the rate of diffusion of the phosphate molecules across the surrounding layer and in the internal pores of the adsorbent (Fe-CAC). Probably, this is the reason why phosphate adsorption capacity increases with increasing temperature of the solution. From the above reason, the reaction process of phosphate with Fe-CAC is endothermic.

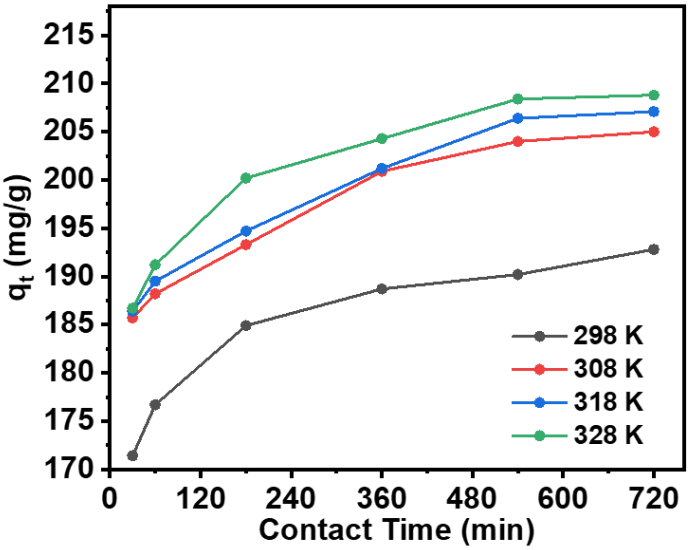

Figure 7: Effect of Temperature on phosphate adsorption (initial concentration of 250 mg/L, pH, 4, adsorbent dose 0.05g, and, agitation speed: 200 rpm).

IV. Regeneration Studies of Fe-AC Adsorbent

Phosphate adsorption regeneration experiments on Fe-CAC produces less greenhouse gas emissions than the production and use of new adsorbents, reduce processing costs and charges, and prevent secondary contamination. The prevailing features of an effective adsorbent in a sustainable way are its regeneration with significant adsorption ability and restoration of its original characteristics upon reuse. The regeneration of the active sites on the activated carbon adsorbent impregnated with iron in cycle usage is proportional to its stability, which is essential for functional application in aqueous solution. This will help to decrease both the environmental risk factors (secondary pollution) as well as the process's operating cost. Therefore, an efficient adsorbent must demonstrate excellent performance in both adsorption and regeneration processes. Similarly, for such studies (Song and Li, 2019; Wu et al., 2019) the adsorbed phosphate was removed with 0.1 M NaOH and deionized water. Furthermore, once a Fe-CAC adsorbent was used, it was rinsed with 0.1 M NaOH and deionized water over several cycles to eliminate the

adsorbed phosphate. Finally, the adsorbent was oven-dried overnight at 80°C and used in aqueous solution to test the reusability of Fe-CAC for phosphate removal. It showed the results of five consecutive cycles of adsorption/desorption in Fig. 8. It may be represented that before reuse, Fe-CAC's adsorption ability was 216.6 mg/g. For the 1st cycle, the significant percentage of phosphate was desorbed (92.8%) with a marginal decrease until the 3rd, while 60.8% was the original desorption capacity at the 5th cycle. The Fe-CAC has a significantly higher regeneration potential and is more robust while being regularly used in aqueous solution for phosphate removal. Therefore, in the aqueous solution, Fe-CAC adsorbent demonstrates excellent performance in both the adsorption and the desorption processes, which is promising for practical applications.

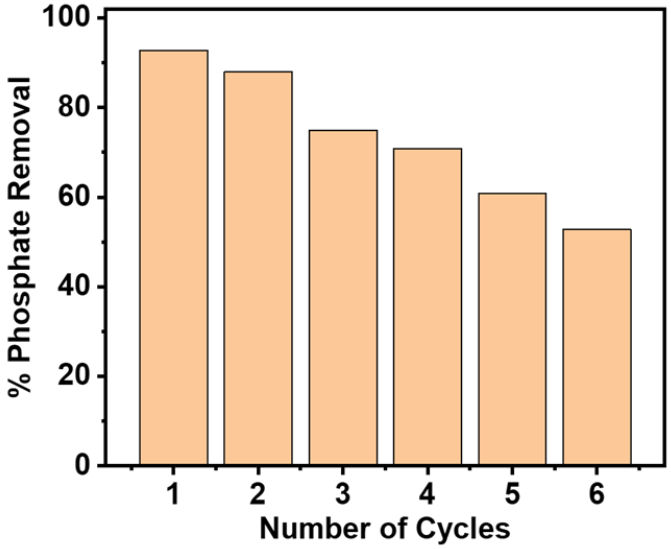

Figure 8: Regeneration performance of prepared Fe-AC (initial concentration: 250 mg/L, pH: 4, Temperature: 298 K, contact time: 9 hrs, adsorbent dosage: 0.05 g, and, agitation speed: 200 rpm).

V. Conclusion

Iron impregnated activated carbon adsorbent (Fe-CAC) was effectively prepared using a simple co-precipitation method. Impregnation of iron on CAC greatly improved phosphate adsorption capacity. Fe-CAC had a high capacity for phosphate adsorption relative to CAC, which could probably be ascribed by its higher binding affinity and selectivity. The pH has a significant effect on phosphate adsorption capacity and removal efficiency, with the maximum phosphate removal achieved in pH 4 for both adsorbents. The adsorption capacity of phosphates on the Fe-CAC increased with increasing temperature. The reaction of phosphate species onto the Fe-CAC adsorbent was rapid in the early stage, with 92% of the phosphate adsorption process was achieved within 60 minutes. the adsorption equilibrium data was better described by the Langmuir isotherm model. Adsorption dynamic study revealed that the adsorption process followed the pseudo-second-order equation. The mechanism was regulated by electrostatic attraction and the exchange of ligands at low pH. The Fe-CAC had significantly higher regeneration capability and more sustainable while repeatedly used for phosphate removal in aqueous solution. Thus, Fe-CAC adsorbent shows excellent performance in the adsorption as well as in desorption processes in the aqueous solution, which is promising for the practical application.

ACKNOWLEDGMENT

I am grateful for the support of the college of environmental science and engineering, state key laboratory of Pollution Control and Resource Reuse all research group members for helping me with the lab experiments. I would like to thank the Ministry of Education of the People's Republic of China, as well as the UN Environment Programme (UNEP), especially UN Environment-Tongji Institute of Environment for Sustainable Development, College of Environmental Science and Engineering, Tongji University, Shanghai 200092, PR China.

References

[1] 1. Yuan, L., et al., Adsorption and mechanistic study for phosphate removal by magnetic Fe3O4-doped spent FCC catalysts adsorbent. Chemosphere, 2019. 219: p. 183-190.

[2] 2. Wan, J., et al., The activated iron system for phosphorus recovery in aqueous environments. Chemosphere, 2018. 196: p. 153-160.

[3] 3. Zhang, L., et al., Removal of phosphate from water by activated carbon fiber loaded with lanthanum oxide. J Hazard Mater, 2011. 190(1-3): p. 848-55.

[4] 4. Ragheb, S.M., Phosphate removal from aqueous solution using slag and fly ash. HBRC Journal, 2019. 9(3): p. 270-275.

[5] 5. Parry, R., Agricultural phosphorus and water quality: A US Environmental Protection Agency perspective. Journal of Environmental Quality, 1998. 27(2): p. 258-261.

[6] 6. Novais, S.V., et al., Phosphorus removal from eutrophic water using modified biochar. Sci Total Environ, 2018. 633: p. 825-835.

[7] 7. Liu, F., et al., Removing phosphorus from aqueous solutions by using iron-modified corn straw biochar. Frontiers of Environmental Science & Engineering, 2015. 9(6): p. 1066-1075.

[8] 8. Sun, J., et al., Nickel toxicity to the performance and microbial community of enhanced biological phosphorus removal system. Chemical Engineering Journal, 2017. 313: p. 415-423.

[9] 9. Mahardika, D., H.S. Park, and K.H. Choo, Ferrihydrite-impregnated granular activated carbon (FH@GAC) for efficient phosphorus removal from wastewater secondary effluent. Chemosphere, 2018. 207: p. 527-533.

[10] 10. Xiong, W., et al., Adsorption of phosphate from aqueous solution using iron-zirconium modified activated carbon nanofiber: Performance and mechanism. J Colloid Interface Sci, 2017. 493: p. 17-23.

[11] 11. Shi, Z.-l., F.-m. Liu, and S.-h. Yao, Adsorptive removal of phosphate from aqueous solutions using activated carbon loaded with Fe(III) oxide. New Carbon Materials, 2011. 26(4): p. 299-306.

[12] 12. Altıntıg, E., et al., Effective removal of methylene blue from aqueous solutions using magnetic loaded activated carbon as novel adsorbent. Chemical Engineering Research and Design, 2017. 122: p. 151-163.

[13] 13. Wang, Z., et al., Equilibrium and kinetics of adsorption of phosphate onto iron-doped activated carbon. Environ Sci Pollut Res Int, 2011. 19(7): p. 2908-17.

[14] 14. Shah, I., et al., Iron impregnated activated carbon as an efficient adsorbent for the removal of methylene blue: regeneration and kinetics studies. PLoS One, 2015. 10(4): p. e0122603.

[15] 15. Ishiwata, T., et al., Removal and recovery of phosphorus in wastewater by superconducting high gradient magnetic separation with ferromagnetic adsorbent. Physica C: Superconductivity and its Applications, 2010. 470(20): p. 1818-1821.

[16] 16. Zhou, Y., et al., Biochar-supported zerovalent iron for removal of various contaminants from aqueous solutions. Bioresource technology, 2014. 152: p. 538-542.

[17] 17. Zong, E., et al., Adsorptive removal of phosphate ions from aqueous solution using zirconia-functionalized graphite oxide. Chemical Engineering Journal, 2013. 221: p. 193-203.

[18] 18. Yoon, S.-Y., et al., Kinetic, equilibrium and thermodynamic studies for phosphate adsorption to magnetic iron oxide nanoparticles. Chemical Engineering Journal, 2014. 236: p. 341-347.

[19] 19. Tu, Y.-J., et al., Application of magnetic nano-particles for phosphorus removal/recovery in aqueous solution. Journal of the Taiwan Institute of Chemical Engineers, 2015. 46: p. 148-154.

[20] 20. Renman, A. and G. Renman, Long-term phosphate removal by the calcium-silicate material Polonite in wastewater filtration systems. Chemosphere, 2010. 79(6): p. 659-64.

[21] 21. Boujelben, N., et al., Phosphorus removal from aqueous solution using iron coated natural and engineered sorbents. Journal of hazardous materials, 2008. 151(1): p. 103-110.

[22] 22. Chang, Q., W. Lin, and W.C. Ying, Preparation of iron-impregnated granular activated carbon for arsenic removal from drinking water. J Hazard Mater, 2010. 184(1-3): p. 515-22.

[23] 23. Jung, K.W., et al., Kinetic study on phosphate removal from aqueous solution by biochar derived from peanut shell as renewable adsorptive media. International Journal of Environmental Science and Technology, 2015. 12(10): p. 3363-3372.

[24] 24. Bacelo, H., et al., Performance and prospects of different adsorbents for phosphorus uptake and recovery from water. Chemical Engineering Journal, 2020. 381.

[25] 25. Thermally treated aluminium waste-filings, a low cost and efficient adsorbent for phosphorus removal from water. Global NEST Journal, 2018. 20(3): p. 488-496.

[26] 26. Boujelben, N., et al., Phosphorus removal from aqueous solution using iron coated natural and engineered sorbents. J Hazard Mater, 2008. 151(1): p. 103-10.

[27] 27. Yang, Q., et al., Effectiveness and mechanisms of phosphate adsorption on iron-modified biochars derived from waste activated sludge. Bioresour Technol, 2018. 247: p. 537-544.

[28] 28. Yihunu, E.W., et al., Preparation, characterization and cost analysis of activated biochar and hydrochar derived from agricultural waste: a comparative study. SN Applied Sciences, 2019. 1(8).

[29] 29. Ren, Z., L. Shao, and G. Zhang, Adsorption of Phosphate from Aqueous Solution Using an Iron–Zirconium Binary Oxide Sorbent. Water, Air, & Soil Pollution, 2012. 223(7): p. 4221-4231.

[30] 30. Wilfert, P., et al., The Relevance of Phosphorus and Iron Chemistry to the Recovery of Phosphorus from Wastewater: A Review. Environ Sci Technol, 2015. 49(16): p. 9400-14.

[31] 31. Cheng, S., et al., Comparison of activated carbon and iron/cerium modified activated carbon to remove methylene blue from wastewater. J Environ Sci (China), 2018. 65: p. 92-102.

[32] 32. Mahapatra, K., D. Ramteke, and L. Paliwal, Production of activated carbon from sludge of food processing industry under controlled pyrolysis and its application for methylene blue removal. Journal of Analytical and Applied Pyrolysis, 2012. 95: p. 79-86.

[33] 33. Suresh Kumar, P., et al., Effect of pore size distribution on iron oxide coated granular activated carbons for phosphate adsorption – Importance of mesopores. Chemical Engineering Journal, 2017. 326: p. 231-239.

[34] 34. Long, F., et al., Removal of phosphate from aqueous solution by magnetic Fe–Zr binary oxide. Chemical Engineering Journal, 2011. 171(2): p. 448-455.

[35] 35. Ding, L., et al., Adsorptive characteristics of phosphate from aqueous solutions by MIEX resin. J Colloid Interface Sci, 2012. 376(1): p. 224-32.

AUTHORS

First Author – Bayuh Abuhay Kibret, Master candidate student, Tongji University, College of Environmental Science and Engineering, Email: bayeabu2055@gmail.com, China, Mobile: +86 13262620942

Second Author – Ye Wu, Master candidate student, Tongji University, College of Environmental Science and Engineering Email: 1923981404@qq.com

Third Author – Mengist Minale Tashu, Email: mengew3c@gmail.com

Correspondence Author – Fengting Li (Professor)
Email: fengting@tongji.edu.cn, china, mobile:+862165987790